Noise resistance of stochastic image binding algorithms on the base of mutual information

Alexander Tashlinskii
Radio Engineering Department
Ulyanovsk State Technical University
Ulyanovsk, Russia
tag@ulstu.ru

Radik Ibragimov
Radio Engineering Department
Ulyanovsk State Technical University
Ulyanovsk, Russia
ibragimow.it@gmail.com

Galina Safina
National Research Moscow State University of Civil Engineering
Moscow, Russia
minkinag@mail.ru

***Abstract*—Based on the mutual information of Shannon, Tsallis and Renyi, relay stochastic algorithms for image binding were synthesized and their stability and accuracy were studied.**

Kewwords—image binding, stochastic procedure, geometric deformation, mutual information, Shannon, Tsallis, Renyi

I. Introduction

The need to image binding arises when solving various practical problems, such as analyzing satellite and medical images, calculating the trajectory of unmanned vehicles, and many others. In this case, the images may be distorted as a result of various interference, which introduces additional a priori uncertainty. In such conditions, good results are shown by relay stochastic image binding algorithms [1], using such measures of image similarity as mutual information (MI) as an objective function.

II. Problem Statement and Algorithm Synthesis

The paper considers the effectiveness of using three types of MI: Shannon [2], Renyi [3] and Tsallis [4] as a quality objective function for image binding algorithms synthesized based on the mathematical apparatus of stochastic gradient adaptation [5]. The aim of the work is to synthesize image binding algorithms based on MI and a comparative study of the stability and accuracy of binding parameter estimates in the conditions of different intensity noise.

For the synthesis of algorithms, expressions were found for estimating the probability density (PD) and the joint PD of the original and deformed images using the Parsen window method [6], and calculation formulas for the derivatives of the entropy of MI according to the estimated binding parameters were analytically obtained, assuming the use of a special case of the general affine model as a model of image deformations, the similarity model [7], whose parameters there are shifts h_x and h_y along the base axes of the images, the angle of rotation φ and the scale factor κ.

III. Experimental Results

The studies were carried out on real and simulated images. Examples of the results were obtained on synthesized images obtained using the wave model [8] and having a brightness distribution close to Gaussian, as well as on satellite images of the optical range. For equal conditions in the examples below, the deformed image was obtained from the original one with the deformation parameters: h_x=-3.4; h_y=4.2; φ=5.1; κ=1.07. As indicators by which the efficiency of algorithms synthesized based on different types of MI were compared, the resistance to noise and error in the vector of estimates of deformation parameters were used. Stability was defined as the proportion of estimation failures per 30 implementations of the algorithm. The error was characterized by the variance of the Euclidean mismatch distance (EMD) [9], which integrally describes the vector of estimates of deformation parameters. The studies were carried out in the range of signal/additive noise ratio q from 5.5 to 0.5 (according to variances).

Fig. 1 shows an example of a simulated (Fig. 1a) and deformed noisy image at q=1 (Fig. 1b). In Fig. 1c and Fig. 1d their brightness distribution are presented. It can be seen that as the noise increases, the brightness distribution normalizes.

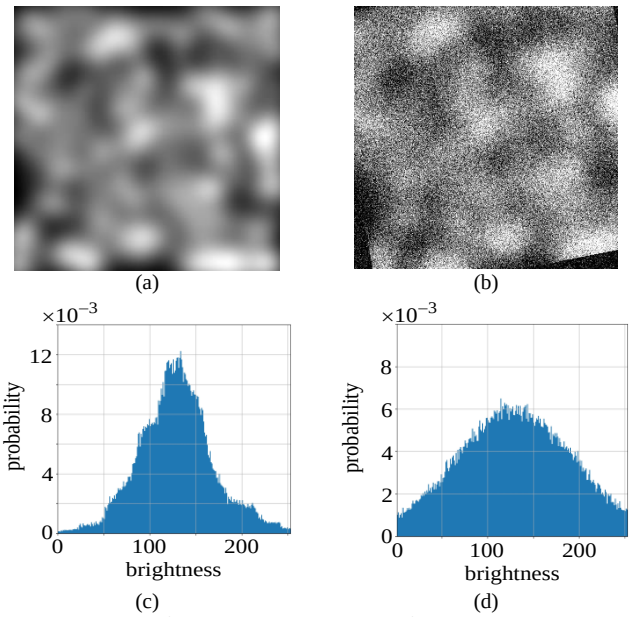

Fig. 1. Example of simulated and noisy deformed images and their brightness probability distributions

The dependence of failure proportion on q is shown in Fig. 2a. Here, as well as in Fig. 3a and Fig. 5, the red curve shows the results of the algorithm synthesized on the basis of the Tsallis MI, the green one shows the Shannon MI, and the blue one the Renyi MI. It can be seen that the Tsallis MI has the least stability among the investigated objective functions. Already at q=4, a sharp increase in the share of failures begins. The best stability was shown by the algorithm based on Renyi MI, whose failures begin at q less than 2. The variance of the estimation error is shown in Fig. 2b, from which it can be seen that the algorithm based on the Renyi MI has the smallest error, and the largest error has the Tsallis MI. In this case, the loss is more than 1.5 times. The algorithm based on Shennov MI loses about 20 %.

The conclusion about the best stability and accuracy of the algorithm based on the data is also confirmed by the

normalized (to the maximum) dependences of various types of MI on the displacement along one of the coordinate axes (Fig. 3a). It can be seen that the rate of decline from the maximum for Renyi MI is less, it provides more information and, accordingly, better results in noise and in conditions of geometric deformations. An example of the curves for Renyi MI with different values of q is shown in Fig. 3b. Here the blue curve corresponds to the ratio 5.5, the green to 3, the red to 1. It can be seen that at the boundary of the displacement range the difference is less than 1.1 times, whereas for Shannon MI is 1.7 times, and for Tsallis MI is 2.6 times.

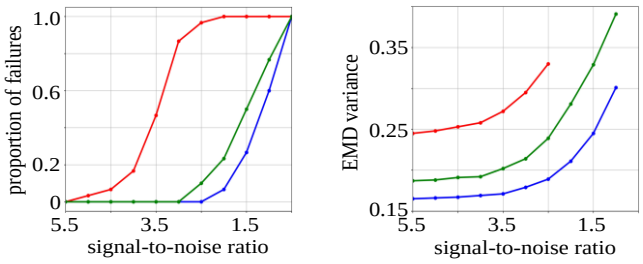

(a) (b)

Fig. 2. The proportion of evaluation failures and the variance of estimates for different types of MI in the simulated image

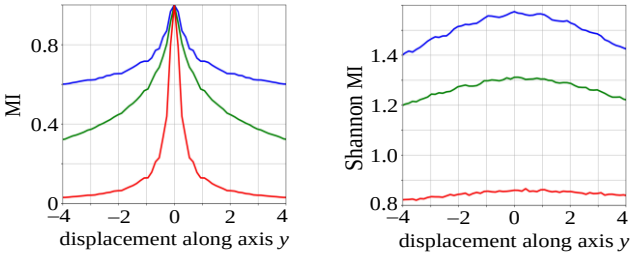

(a) (b)

Fig. 3. The dependence of MI on the displacement

In Fig. 4 the examples of a satellite image of the Volga River water area (Fig. 4a), a deformed noisy image (Fig. 4b), and the distribution of their brightness (Fig. 4c and Fig. 4d) are shown. It can be seen that the brightness distribution of the real image is very different from the Gaussian one. The dependence of failure proportion on q is shown in Fig. 5a, and the EMD variances are shown in Fig. 5b. In general, the qualitative results are close to those described above. The best results were also shown by the algorithm based on Renyi MI, however, as can be seen from the figures, the use of Shannon MI in this case gave similar results.

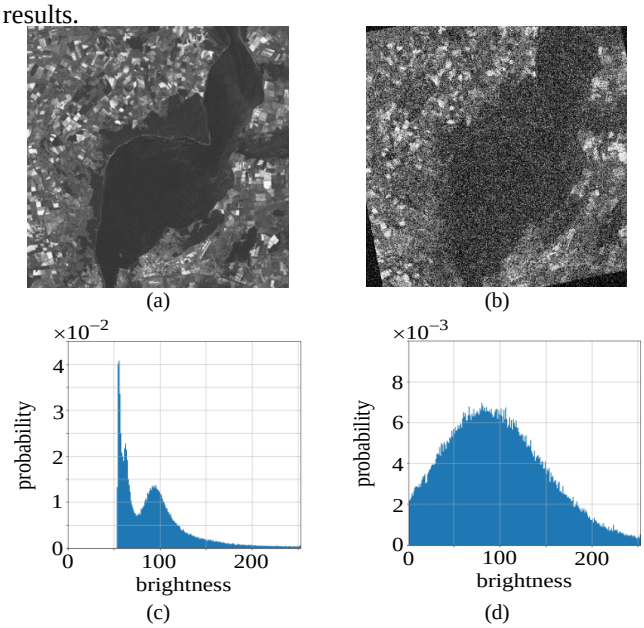

(a) (b)

(c) (d)

Fig. 4. Example of real and noisy deformed images and their brightness probability distributions

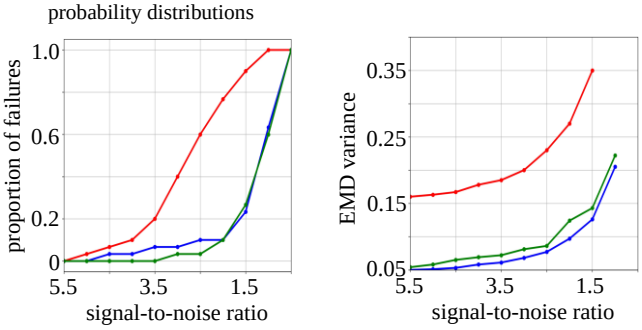

(a) (b)

Fig. 5. The proportion of estimation failures and the variance of estimates for different types of MI on a real image

IV. Conclusion

The approbation of image binding algorithms synthesized on the basis of Shannon, Tsallis and Renyi MI showed that the least stability (both in terms of the proportion of evaluation failures and the EMD variance) to additive noise was shown by the algorithm based on Tsallis MI. When evaluating deformations of images with a brightness distribution close to Gaussian, noise resistance is lower than in higher-frequency images with a complex pixel brightness distribution. In particular, in the examples given for the simulated image, 100 % of evaluation failures were observed for the MI Tsallis algorithm with a signal-to-noise ratio of about 2, whereas in the real image, failures with the same noise were about 30 %. Note also that in comparison with algorithms based on Shannon and Renyi MI, the usage of Tsallis MI requires 1.3-1.4 times more iterations to achieve convergence of the binding estimates.

Acknowledgment

The work was supported by the Russian Science Foundation according to research projects No. 22-21-00513, https://rscf.ru/en/project/22-21-00513/.

References

[1] Tashlinskii, A. Application of Renyi Mutual Information in Stochastic Referencing of Multispectral and Multi-temporal Images / A. Tashlinskii, R. Ibragimov, G. Safina // IEEE Xplore. – 2022. – Vol. 21992095. – P. 1-6.

[2] Hongyang, J. Neonatal Fundus Image Registration and Mosaic Using Improved Speeded Up Robust Features Based on Shannon Entropy / J. Hongyang, G. Mengdi, Y. Kang, Z. Dongdong, M. He, Q. Wei // Annual International Conference of the IEEE Engineering in Medicine & Biology Society (EMBC). – 2021. – P. 3004-3007.

[3] Meisen, P. Medical Image Registration Based on Renyi's Quadratic Mutual Information / P. Meisen, F. Zhang // IETE Journal of Research. – 2020. – P. 1–9.

[4] Sparavigna, C. On the Role of Tsallis Entropy in Image Processing / C. Sparavigna // International Scientific Research Journal. – 2015. – Vol. 1 (6). – P. 16-24.

[5] Tashlinskii, A.G. Pseudogradient Estimation of Digital Images Interframe Geometrical Deformations / Tashlinskii A.G. // Vision Systems: Segmentation & Pattern Recognition. – 2007. – P. 465-494.

[6] Mussa, H. The Parzen Window method: In terms of two vectors and one matrix / H. Mussaa, J. Mitchell, A. Afzalb // Pattern Recognition Letters. – 2015. – Vol. 63. – P. 30-35.

[7] Gonzalez, R.C. Digital image processing / R.C. Gonzalez, E. Woods. – London: Pearson Publisher, 2018. – 1019 p.

[8] Krasheninnikov, V.R. Fundamentals of image processing theory / V.R. Krasheninnikov. – Uljanovsk: IlGTU, 2003. – 152 p. (In Russian).

[9] Tashlinskii, A.G. Pseudogradient optimization in the estimation of geometric interframe image deformations / A.G. Tashlinskii, G.L. Minkina // Pattern Recognition and Image Analysis. – 2008. – Vol. 18 (4). – P. 706-711.